Received: 06 December 2021 | Revised: 28 March 2022 | Accepted: 31 March 2022
DOI: 10.22034/ecc.2022.328320.1320
Eurasian Chemical Communications
SAMI

FULL PAPER

Single crystal X-ray structure analysis and DFT studies of 3-hydroxyl-1,7,7-trimethyl-3-[5-(4-methylphenyl)-1,3,4-oxadiazol-2-yl]bicycle [2.2.1]heptan-2-one

Ghasem Moghadam[a,f] |Ali Ramazani[b,c,*] |Fatemeh Zeinali Nasrabadi[d,*] |Hamideh Ahankar[e] | Katarzyna Ślepokura[g] |Tadeusz Lis[g] |Ali Kazami Babaheydari[h]

[a]*Department of Chemistry, University of Isfahan, P O Box 81746-73441, Isfahan, Iran*

[b]*Department of Chemistry, University of Zanjan, Zanjan 4537138791, Iran*

[c]*Department of Biotechnology, Research Institute of Modern Biological Techniques (RIMBT), University of Zanjan, Zanjan 4537138791, Iran*

[d]*Department of Chemistry, Faculty of Valiasr, Tehran Branch, Technical and Vocational University, Tehran, Iran*

[e]*Department of Chemistry, Abhar Branch, Islamic Azad University P O Box 22, Abhar, Iran*

[f]*Young Researchers and Elites Club, Islamic Azad University, Shahrekord branch, Shahrekord, Iran*

[g]*Faculty of Chemistry, University of Wrocław, 14 Joliot-Curie St., 50-383 Wrocław, Poland*

[h]*Department of Pharmaceutical Chemistry, Tehran Medical Sciences, Islamic Azad University, Tehran, Iran*

***Corresponding Author:**
Ali Ramazani and Fatemeh Zeinali Nasrabadi
Email: aliramazani@gmail.com, f_pzeinali@yahoo.com
Tel.: +98 (0243) 305257

Single crystal X-ray structure analyses of 3-Hydroxyl-1,7,7-trimethyl-3-[5-(4-methyl phenyl)-1,3,4-oxadiazol-2-yl]bicycle [2.2.1] heptan-2-one was performed. In addition, the computational investigations such as optimization energy, infrared spectra, the frontier orbitals of HOMO, LUMO, HOMO-1, and LUMO+1 analysis, molecular electrostatic potential plots, heat capacity, entropy, and charge distribution were performed on the products at DFT/B3LYP methods. The comparison between the experimental and theoretical results demonstrated that these two results are in good agreement.

KEYWORDS

Single crystal X-ray analysis; molecular structure; DFT calculations; 1,3,4-oxadiazole; (1*R*)-(-)-campherchinon.

Introduction

Multicomponent reactions (MCRs) can be regarded as an effective and robust means in today's synthetic organic chemistry; this is owing to the good qualities like atom economy and good reaction design, as well as the possibility of constructing target compounds by introducing a number of components in one single chemical incident [1]. Also, products purification resulted from MCR is usually not complicated as the whole organic reagents are applied and can be inserted into the targeted compound [2-4]. MCRs, resulting in notable heterocyclic scaffolds, are especially suitable for constructing varied "druglike" molecules chemical libraries. Isocyanide-based MCRs are particularly significant in such an area [5,6]. Of MCRs to date, the ones based on isocyanides are the most effective reactions. Isocyanide-based multicomponent reactions (IMCRs) have been of much recent research interest

due to their interesting synthetic potential, implementation ease, and the possibility of molecular variety in the combinatorial chemistry field [7,8].

Camphor and its derivatives are considered as one of the most widely used enantiopure building blocks, agents shift reagents in the NMR spectroscopy, and ligands in a wide range of asymmetric reagents as well as catalysts [9-11]. Camphorquinone, 6-oxocamphor, also known as 2,3-bornanedione is a photo initiator applied in curing dental composites [12]. (1*R*)-(–)-Campherchinon (Figure 1) is one of the camphor derivatives, which can be used as a chiral starting material for the preparation of diverse and different chiral organic compound [13,14]. Likewise, various camphor derivatives have been used in asymmetric hydrogenation reactions [15,16]. Moreover, some of the camphor derivatives demonstrate fascinating biological and pharmaceutical activities. By the way, camphorsulphonylbenzimidazoles contain an anti-bacterial [17], and anti-spasmodic effect has been applied in the pharmaceutical field [18].

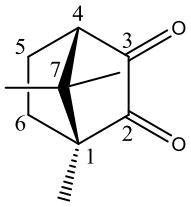

FIGURE 1 Molecular structure of (1*R*)-(–)-Campherchinon

Over past years, the substantial research has been carried out on various types of oxadiazoles. Especially, organic compounds including 1,3,4-oxadiazole base have been demonstrated to have a vast array of pharmacological and therapeutic activities. A group of 1,3,4-oxadiazoles have revealed myorelaxant, painkiller, hypotensive, and antiemetic activities [19-21]. A suitable procedure has been previously reported for the synthesis of 1,3,4-oxadiazoles [22,23].

Theoretical chemistry is a part of chemistry with the simulation of molecules and atoms which can help researchers to find better chemical structures. It assists the experimental chemists to predict molecular structure [24], identify the correlation between the chemical structures and molecular properties [25], to find the chemical approaches for synthesis of organic and inorganic compounds [26], drug design [27], *etc*. Hartree-Fock calculation (abbreviated as HF) is a common kind of *ab initio* method. In HF methods, the central field approximation is the early approximation. By definition, the coulombic electron-electron excretion is inverted by integrating the repulsion period. A strong method leading to the quantum chemistry for the prediction of the electron structure of molecules is Density functional theory (DFT). The DFT methods are being more and more useful. The results deduced by DFT methods are comparable to the results presented by *ab initio* methods. The most popular of DFT model is B3LYP [5]. Due to our interest in the synthesis of heterocycle compounds [28,29], single crystal X-ray structure [30-32] and computational chemistry as DFT studies [33-39], in the current study, we reported a theoretical investigation, and compared it with the experimental analysis such as FT-IR spectra, the frontier orbitals of HOMO, LUMO, HOMO-1, and LUMO+1 analysis, heat capacity, entropy, charge distribution and molecular electrostatic plots in association with the compound mentioned earlier.

Experimental

The 3-hydroxyl-1,7,7-trimethyl-3-[5–(4-methylphenyl)–1,3,4-oxadiazol–2–

yl]bicyclo[2.2.1]heptan-2-one (**1A**) was obtained using the procedure described in a previous study [40]. The molecular structure of **1A** was displayed in Figure 2. Colorless single crystals were grown by gradual vaporization of its petroleum ether/methanol (1:1) solution. The colorless single crystals were filtered, washed with a cold mixture of petroleum ether/methanol (1:1) and dried at room temperature.

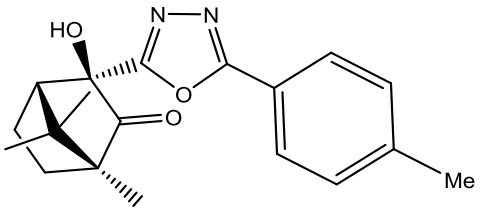

FUGURE 2 Molecular structure of 1A

Single crystal X-ray diffraction of 1A

We measured the crystallographic measurement on an Xcalibur R κ-geometry automated four-circle diffractometer accompanied by a CCD camera Ruby and graphite-monochromatized Mo*K*α radiation (*λ* = 0.71073 Å). The data collection was conducted at 80(2) K using the *Oxford-Cryosystems* cooler. Data were corrected for Lorentz and polarization impacts. Xcalibur R software, *CrysAlisPro* was applied to gather the data, refine cell, reduce, and analyze the data [41]. Using direct methods with the *SHELXS97* program, we solved the structure [42], refined it by a full-matrix least-squares technique with *SHELXL2013* [42], and considered anisotropic thermal parameters for non-H atoms. The whole H atoms were detected in various Fourier maps and refined isotropically. As for the final refinement stages, the C-bonded H atoms experienced repositioning in their computed positions and were refined applying a riding model, with C–H = 0.95–1.00 Å, and Uiso(H) = 1.2Ueq(C) for CH and CH2, as well as 1.5U_{eq}(C) for CH_3. Hydroxyl H atom was refined without restriction. *DIAMOND* program was utilized to make figures [43]. Details of the conditions for the data collection and structures refinements are given in the crystallographic information file (CIF) deposited with The Cambridge Crystallographic Data Centre (www.ccdc.cam.ac.uk/; deposition number CCDC-2089303) and provided as ancillary data.

Crystal data

$C_{19}H_{22}N_2O_3$, *M*r = 326.38, colorless block, crystal size 0.44 × 0.43 × 0.41 mm, trigonal, space group $P3_2$, *a* = 11.050(3), *c* = 12.319(3) Å, *V* = 1302.7(8) Å^3,T = 80(2) K, Z = 3, *μ* = 0.09 mm^{-1} (for Mo Kα, λ = 0.71073 Å), the empirical absorption correction (multi-can), T_{min} = 0.990, T_{max} = 1.000, 10018 reflections measured, 5223 unique (R_{int} = 0.020), 5025 observed ($I > 2\sigma(I)$), $(\sin\theta/\lambda)_{max}$ = 0.746 Å^{-1}, 225 parameters, 1 restraint, *R* = 0.035 (observed refl.), w*R* = 0.091 (all refl.), GOOF = *S* = 1.03, ($\Delta\rho_{max}$) = 0.35, and ($\Delta_{\rho min}$) = −0.25 e Å^{-3}. Absolute configuration was known.

Computational details

The theoretical study was calculated using the Gaussian 09W software package [44]. The DFT method get the Becke3 exchange functional completed with Lee, Yang, Parr (LYP) correlation functional [45,46]. The geometry optimizations were achieved by HF and DFT/B3LYP methods as well as 6-31G, 6-311G* basis sets, respectively, to take the closest structure. The wavenumbers were calculated at B3LYP/6-311G*. It was indicated by specializing part of Gauss View 6.0 software which reveals the FT-IR spectrum of the vibration models [47]. The molecular

geometries were fully optimized and shown at B3LYP/6-311G*.

Results and discussion

To develop powerful methods for providing heterocyclic compounds included in our ongoing program, the synthesis of 1,3,4-oxadiazoles by a three-component condensation of (*N*-isocyanimino)triphenylphosphorane, 4-methylbenzoic acid, and (1*R*)-(-)-campherchinon was tested. The FT-IR, ^{1}H NMR, and ^{13}C NMR spectroscopy was used to confirm the product's structure [40].

The molecular structure of **1A** was optimized using B3LYP/6-311G* (Figure 3). The energy of optimization, frontier orbitals of HOMO, LUMO, HOMO-1, LUMO+1, and energy gap were obtained within B3LYP/6-311G* as displayed in Table 1.

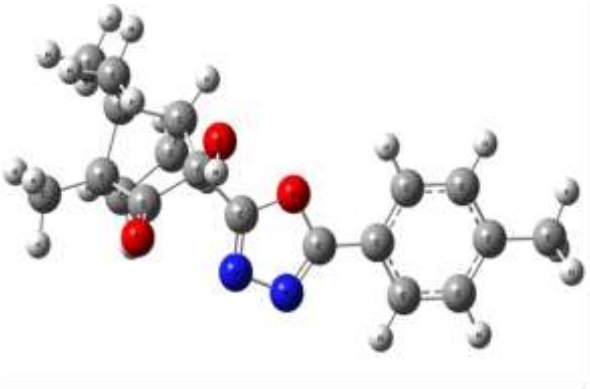

FIGURE 3 The molecular structure of **1A** optimized using B3LYP/6-311G (d,p)

The FT-IR spectrum of the molecule **1A** was obtained by B3LYP/6-311G* method and basis set. The FT-IR diagrams of compound **1A** were designed by animation option of Gauss view 6.0 software, as illustrated in Figure 4. The comparison between the experimental [40] and theoretical FT-IR spectra results demonstrate that these two results are in good agreement.

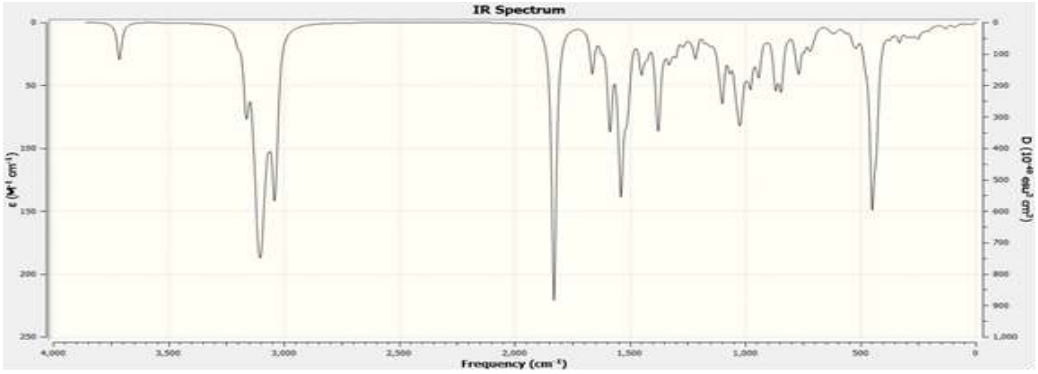

FIGURE 4 The computational FT-IR spectrum for **1A** calculated by B3LYP/6-311G*

Frontier high occupied molecular orbital (HOMO) and low unoccupied molecular orbital (LUMO) of 1A plotted in 3D by B3LYP/6-311G* method and basis sets are displayed in Figure 5. Optimization energy, heat capacity, entropy, HOMO, LUMO, HOMO-1, LUMO+1, and the energy gap for compound **1A** are depicted in Table 1. With a vector in three dimensions, the dipole moment can be revealed by molecular charge distribution. Thus, it can be suitable as an explanator to determine the movement of electric charges throughout the molecules [48]. The nucleophilicity and electrophilicity properties, dipole moments, and the molecules interactions with each other can be predicted

by charge distribution in the molecules. The molecular electrostatic potential (MEP), electron density surface plots (ESP), and the molecular charge distributions on the surface of the compound **1A** calculated at B3LYP/6-311G* method and basis set are depicted in Figure 5. According to Figure 6, the oxadiazole ring, carbonyl, and hydroxyl groups are negative (-) regions (red area), and methyl group and phenyl ring are positive (+) regions (green area). The Mullikan charge distribution plots of compound **1A** calculated by B3LYP/ 6-311G* are shown in Figure 7, confirming the obtained results by MEP and ESP contour plots.

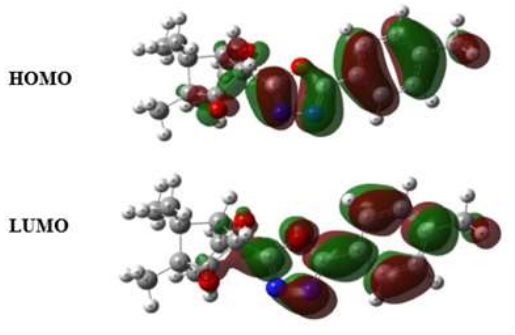

FIGURE 5 The 3D plot of frontier HOMO and LUMO orbitals of **1A** using B3LYP/6-311G* method and basis sets

TABLE 1 Some molecular orbital properties and optimization energy for 1A calculated by B3LYP/6-311G*

E (Thermal) KCal/Mol	CV Cal/Mol-Kelvin	S Cal/Mol-Kelvin	HOMO	HOMO-1	LUMO	LUMO+1	GAP	GAP +1,-1
251.725	84.677	152.322	-0.24237	-0.25376	-0.05715	-0.03579	-0.18522	-0.21797

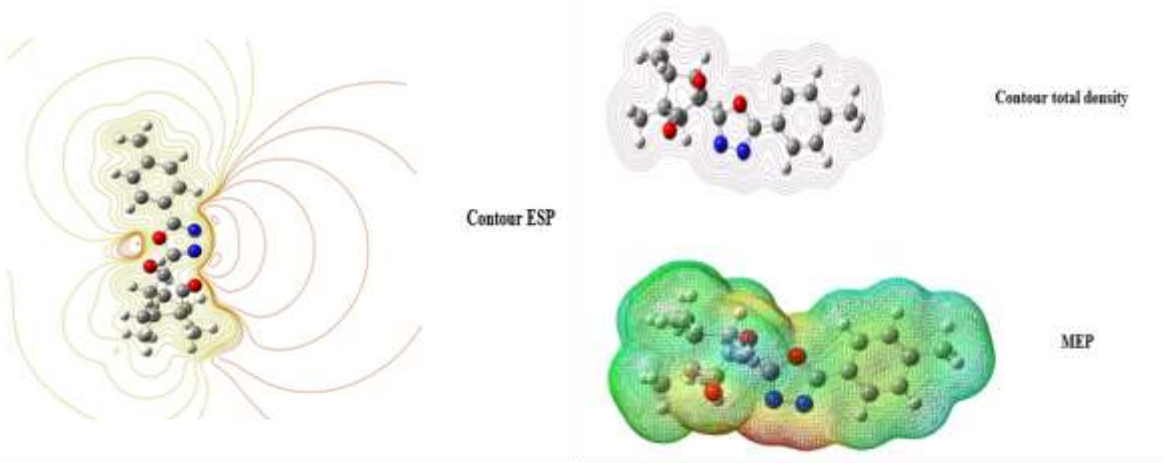

FIGURE 6 ESP, Contour total density, and MEP of the compound **1A** shown as charge distributions on the surface, calculated at B3LYP/6-311G* method and basis set

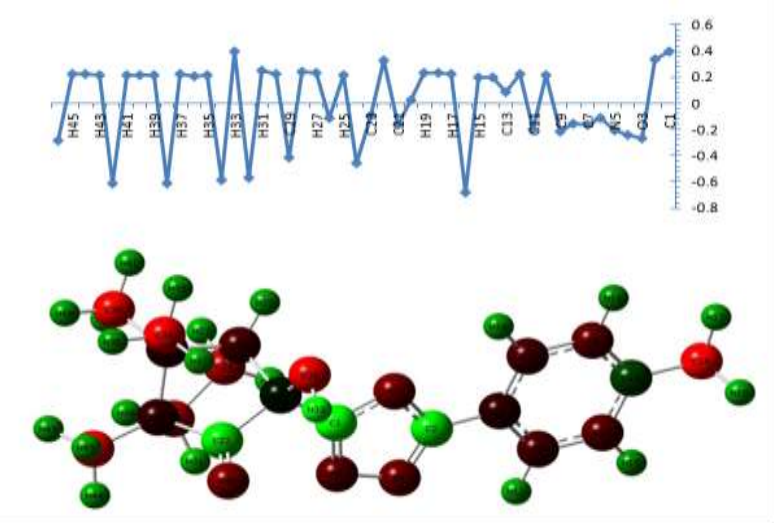

FIGURE 7 The Mullikan charge distribution plots of compound **1A** calculated by B3LYP/ 6-311G*

X-ray crystal structure

The molecular structure of **1A** was determined with the use of X-ray crystallography (Figure 8). The compound crystallizes in the chiral trigonal $P3_2$ space group. As indicated in Table 2, (4-methylphenyl)–1,3,4-oxadiazole fragment of the molecule is almost planar, with the p-tolyl being only slightly twisted relative to the oxadiazole ring (C14—C13—C12—O1 torsion angle of 18.8(2)°). To this planar part, bicyclic camphor moiety is linked *via* the chiral atom C3 (absolute configuration *S*). The C3-bound OH group is an acceptor of weak intramolecular C–H···O contact (Figure 8), and a donor of intermolecular N–H···O hydrogen bond (Table 3). As a result of the latter interactions between molecules resulting from the action of threefold screw axis 3_2, helical chains (running down the *c*-axis) are shaped in the crystal of **1A** (Figure 9).

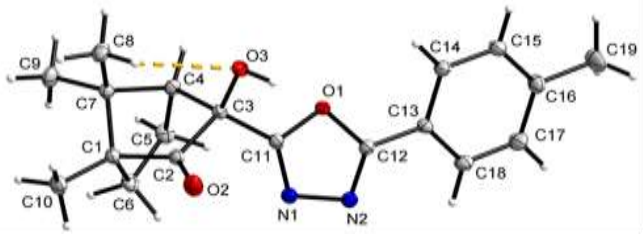

FIGURE 8 X-Ray structure of **1A**, indicating the atom-numbering scheme and the intramolecular C–H·· O hydrogen bond (light orange dashed line). Displacement ellipsoids are drawn at the 50 % probability level

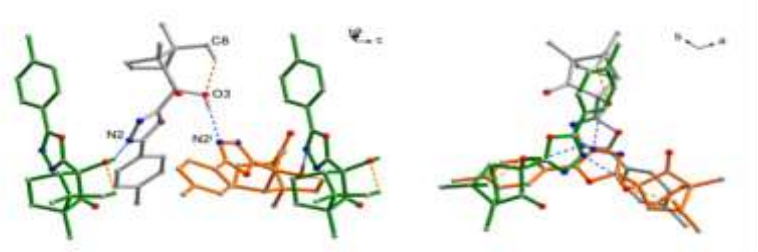

FIGURE 9 Helical chain (side and top view), running down the *c*-axis, built up from molecules of **1A** joined *via* intermolecular N–H···O hydrogen bonds (blue dashed lines). Symmetry code (i) $-x+y, -x, z+1/3$

TABLE 2 Selected geometric parameters (Å, º) for 1A

O1—C11	1.3622(17)
O1—C12	1.3643(17)
N1—N2	1.4149(18)
N1—C11	1.2882(19)
N2—C12	1.2990(19)
C11—O1—C12	102.75(11)
C11—N1—N2	105.81(12)
C12—N2—N1	106.27(12)
O3—C3—C11—O1	−51.18(16)
C2—C3—C11—O1	−173.48(12)
C4—C3—C11—O1	74.24(16)
C14—C13—C12—O1	18.8(2)

TABLE 3 Geometry of hydrogen bonds (Å, º) in 1A

D*—H···*A	***D*—H**	**H···*A***	***D*···*A***	***D*—H···*A***
O3—H3···N2^{i}	0.89(3)	2.02(3)	2.8701(18)	159(3)
C6—H6*B*···O2^{ii}	0.99	2.21	3.192(2)	172
C8—H8*B*···O3	0.98	2.32	2.950(2)	121

Symmetry codes: (i) −x+y, −x, z+1/3; (ii) −y+1, x−y+1, z−1/3

Conclusion

In this study, DFT calculation analysis and comparison between theoretical and experimental for **1A** were obtained. The frontier orbitals of HOMO and LUMO, thermodynamic properties, charge distribution, spectroscopic FT-IR, ESP, and MEP studies were carried out using B3LYP methods and 6-311G(d,p) basis set. According to the ESP and MEP plots illustrated that oxadiazole ring and carbonyl/hydroxyl group are negative (-) region (red area) and methyl group and phenyl ring are positive (+) region (green area). Based on the results, the molecular geometry parameter represents a good agreement with the experimental results.

Acknowledgements

This research was supported by "Zanjan University".

Orcid:

Ali Ramazani:
https://www.orcid.org/0000-0003-3072-7924

Hamideh Ahankar:
https://www.orcid.org/0000-0002-2717-8920

References

[1] R.W. Armstrong, A.P. Combs, P.A. Tempest, S.D. Brown, T.A. Keating, *Acc. Chem. Res.*, **1996**, *29*, 123-131. [Crossref], [Google Scholar], [Publisher]

[2] J. Zhu, H. Bienaymé, *Multicomponent reactions*, John Wiley & Sons, **2006**. [Google Scholar], [Publisher]

[3] B. Baghernejad, M. Talebi, *Asian J. Green Chem.*, **2021**, *5*, 368-377. [Crossref], [Pdf], [Publisher]

[4] M. Fallah-Mehrjardi, M. Foroughi, S.H. Banitaba, *Asian J. Green Chem.*, **2019**, *4*, 75-86. [Crossref], [Google Scholar], [Publisher]

[5] A. Dömling, *Chem. Rev.*, **2006**, *106*, 17-89. [Crossref], [Google Scholar], [Publisher]

[6] I. Yavari, A. Mirzaei, Z. Hossaini, S. Souri, *Mol. Divers.*, **2010**, *14*, 343-347. [Crossref], [Google Scholar], [Publisher]

[7] I. Ugi, B. Werner, A. Dömling, *Molecules*, **2003**, *8*, 53-66. [Crossref], [Google Scholar], [Publisher]

[8] I. Yavari, Z. Hossaini, M. Sabbaghan, *Mol. Divers.*, **2006**, *10*, 479-482. [Crossref], [Google Scholar], [Publisher]
[9] T. Money, *Nat. Prod. Rep.*, **1985**, *2*, 253-289. [Crossref], [Google Scholar], [Publisher]
[10] W. Oppolzer, *Tetrahedron,* **1987**, *43*, 1969-2004. [Crossref], [Google Scholar], [Publisher]
[11] W. Oppolzer, *Pure Appl. Chem.*, **1990**, *62*, 1241-1250. [Crossref], [Google Scholar], [Publisher]
[12] J. Jakubiak, X. Allonas, J.P. Fouassier, A. Sionkowska, E. Andrzejewska, L.Å. Lindèn, J.F. Rabek, *Polymer*, **2003**, *44*, 5219-5226. [Crossref], [Google Scholar], [Publisher]
[13] M. Kitamura, S. Suga, K. Kawai, R. Noyori, *J. Am. Chem. Soc.*, **1986**, *108*, 6071-6072. [Crossref], [Google Scholar], [Publisher]
[14] M. Kitamura, S. Suga, H. Oka, R. Noyori, *J. Am. Chem. Soc.*, **1998**, *120*, 9800-9809. [Crossref], [Google Scholar], [Publisher]
[15] T. Bunlaksananusorn, K. Polborn, P. Knochel, *Angew. Chem. Int. Ed.*, **2003**, *42*, 3941-3943. [Crossref], [Google Scholar], [Publisher]
[16] T. Bunlaksananusorn, P. Knochel, *J. Org. Chem.*, **2004**, *69*, 4595-4601. [Crossref], [Google Scholar], [Publisher]
[17] M. Hasan, H. Masood, K. Naeema, M. Zia-ul-Haq, *Turk. J. Chem.*, **1996**, *20*, 228-233. [Crossref], [Google Scholar], [Publisher]
[18] A.G. Martinez, E.T. Vilar, A.G. Fraile, S. de la Moya Cerero, C.D. Morillo, *Tetrahedron*, **2005**, *61*, 599-601. [Crossref], [Google Scholar], [Publisher]
[19] B.S. Holla, R. Gonsalves, S. Shenoy, *Eur. J. Med. Chem.*, **2000**, *35*, 267-271. [Crossref], [Google Scholar], [Publisher]
[20] I.R. Baxendale, S.V. Ley, M. Martinelli, *Tetrahedron*, **2005**, *61*, 5323-5349. [Crossref], [Google Scholar], [Publisher]
[21] F. Palacios, D. Aparicio, G. Rubiales, C. Alonso, J.M. de los Santos, *Curr. Org. Chem.*, **2009**, *13*, 810-828. [Crossref], [Google Scholar], [Publisher]
[22] A. Ramazani, Y. Ahmadi, N. Fattahi, H. Ahankar, M. Pakzad, H. Aghahosseini, A. Rezaei, S.T. Fardood, S.W. Joo, Phosphorus, *Sulfur Silicon Relat. Elem.*, **2016**, *191*, 1057-1062. [Crossref], [Google Scholar], [Publisher]
[23] H. Ahankar, A. Ramazani, Y. Ahmadi, Phosphorus, *Sulfur Silicon Relat. Elem.*, **2014**, *189*, 914-923. [Crossref], [Google Scholar], [Publisher]
[24] S. Bahçeli, E.K. Sarıkaya, Ö. Dereli, F.P. Özturan, *J. Mol. Struct.*, **2020**, *1216*, 128315. [Crossref], [Google Scholar], [Publisher]
[25] N. Karachi, O. Azadi, R. Razavi, A. Tahvili, Z. Parsaee, *J. Photochem. Photobiol. A*, **2018**, *360*, 152-165. [Crossref], [Google Scholar], [Publisher]
[26] J.R. de Andrade, M.F. Oliveira, R.L.S. Canevesi, R. Landers, M.G.C. da Silva, M.G.A. Vieira, *J. Mol. Liq.*, **2020**, *312*, 113427. [Crossref], [Google Scholar], [Publisher]
[27] M.K. Hazrati, Z. Javanshir, Z. Bagheri, *J. Mol. Graph. Model*, **2017**, *77*, 17-24. [Crossref], [Google Scholar], [Publisher]
[28] H. Ahankar, A. Ramazani, K. Ślepokura, T. Lis, S.W. Joo, *Green Chem.*, **2016**, *18*, 3582-3593. [Crossref], [Google Scholar], [Publisher]
[29] F. Kalantari, A. Ramazani, M.R. Poor Heravi, H. Aghahosseini, K. Ślepokura, *Inorg. Chem.*, **2021**, *60*, 15010-15023. [Crossref], [Google Scholar], [Publisher]
[30] A. Ramazani, H. Ahankar, K. Ślepokura, T. Lis, P.A. Asiabi, M. Sheikhi, F. Gouranlou, H. Yahyaei, *J. Chem. Crystallogr.*, **2020**, *50*, 99-113. [Crossref], [Google Scholar], [Publisher]
[31] A. Ramazani, A. Farshadi, A. Mahyari, K. Ślepokura, T. Lis, M. Rouhani, *J. Chem. Crystallogr.*, **2011**, *41*, 1376-1385. [Crossref], [Google Scholar], [Publisher]
[32] A. Ramazani, H. Ahankar, K. Ślepokura, T. Lis, S. Joo, *J. Struct. Chem.*, **2019**, *60*, 662-670. [Crossref], [Google Scholar], [Publisher]
[33] A. Ramazani, M. Sheikhi, H. Ahankar, M. Rouhani, S.W. Joo, K. Ślepokura, T. Lis, *J. Chem. Crystallogr.*, **2017**, *47*, 198-207. [Crossref], [Google Scholar], [Publisher]
[34] F. Tirgir, M.R. Sabzalian, G. Moghadam, *Des. Monomers Polym.*, **2015**, *18*, 401-412. [Crossref], [Google Scholar], [Publisher]

[35] H. Ahankar, A. Ramazani, H. Saeidian, K. Ślepokura, T. Lis, *J. Struct. Chem.*, **2021**, *62*, 47-57. [Crossref], [Google Scholar], [Publisher]
[36] A. Ramazani, M. Sheikhi, Y. Hanifehpour, P. Asiabi, S. Joo, *J. Struct. Chem.*, **2018**, *59*, 529-540. [Crossref], [Google Scholar], [Publisher]
[37] Z. Hosseinzadeh, M. Khavani, A. Ramazani, H. Ahankar, V. Kinzhybalo, *Eurasian Chem. Commun.*, **2021**, *3*, 35-44. [Crossref], [Google Scholar], [Publisher]
[38] M.N. Sarker, A. Kumer, M.J. Islam, S. Paul, *Asian J. Nanosci. Mate*, **2019**, *2*, 439-447. [Crossref], [Google Scholar], [Publisher]
[39] F. Houshmand, H. Neckoudaria, M. Baghdadi, *Asian J. Nanosci. Mater*, **2018**, *2*, 49-65. [Crossref], [Google Scholar], [Publisher]
[40] A. Ramazani, F.Z. Nasrabadi, B. Abdian, M. Rouhani, *Bull. Korean Chem. Soc.*, **2012**, *33*, 453-458. [Crossref], [Google Scholar], [Publisher]
[41] Crys Alis Pro in Xcalibur software, Agilent Technologies, Yarnton, UK. Oxfordshire, England, **2012**. [Publisher]
[42] G.M. Sheldrick, *Acta Cryst., Sect. A: Found. Crystallogr.*, **2008**, *64*, 112-122. [Crossref], [Publisher]
[43] K. Brandenburg, DIAMOND Version 3.0. Crystal Impact GbR: Bonn, Germany, **2005**. [Google Scholar]
[44] M. Frisch, G. Trucks, H. Schlegel, G. Scuseria, M. Robb, J. Cheeseman, G. Scalmani, V. Barone, B. Mennucci, G. Petersson, H. H. Nakatsuji, X. Li, M. Caricato, A. Marenich, *Wallingford, CT*, **2009**, *32*, 5648-5652.
[45] A.D. Becke, *Phys. Rev. A*, **1988**, *38*, 3098. [Crossref], [Google Scholar], [Publisher]
[46] C. Lee, W. Yang, R.G. Parr, *Phys. Revi. B*, **1988**, *37*, 785. [Crossref], [Google Scholar], [Publisher]
[47] A. Frisch, H.P. Hratchian, R. Dennington II, T. Keith, J. Millam, B. Nielsen, A. Holder, J. Hiscocks, Gaussian, Inc GaussView, John Millam with A., version 5.0., June, **2009**.
[48] G. Moghadam, F. Tirgir, A.H. Reshak, M. Khorshidi, *Mater. Chem. Phys.*, **2019**, *236*, 121780. [Crossref], [Google Scholar], [Publisher]

How to cite this article: Ghasem Moghadam, Ali Ramazani*, Fatemeh Zeinali Nasrabadi*, Hamideh Ahankar, Katarzyna Ślepokura, Tadeusz Lis, Ali Kazami Babaheydari. Single crystal X-ray structure analysis and DFT studies of 3-hydroxyl-1,7,7-trimethyl-3-[5-(4-methylphenyl)-1,3,4-oxadiazol-2-yl]bicycle [2.2.1]heptan-2-one. *Eurasian Chemical Communications*, 2022, 4(8), 759-767. **Link:** http://www.echemcom.com/article_147983.html